Polymer Vol. 37 No. 6, pp. 893–901, 1996

0032-3861/96/$15.00+0.00

Time-resolved *in situ* X-ray scattering studies of aqueous hydroxypropylcellulose solutions

P. A. Keates and G. R. Mitchell*
Polymer Science Centre, J. J. Thomson Physical Laboratory, University of Reading, Whiteknights, Reading RG6 6AF, UK

and E. Peuvrel-Disdier and P. Navard
Ecole des Mines de Paris, Centre de Mise en Forme des Matériaux, URA CNRS 1374, BP 207, 06904 Sophia Antipolis Cedex, France
(Received 25 January 1994; revised 6 April 1994)

The evolution of the global orientation parameter for a series of aqueous hydroxypropylcellulose solutions both during and following the cessation of a steady-state shear flow is reported. Time-resolved orientation measurements were made *in situ* through a novel X-ray rheometer coupled with a two-dimensional electronic X-ray camera, and using an intense X-ray source at the LURE synchrotron. After the cessation of flow, the global orientation decreases from the steady-state orientation level to zero following shear flow at a low shear rate or to a small but finite value after flow at a high shear rate. The decrease of orientation with time shows different behaviour, dependent upon the previously applied shear rate.

(Keywords: hydroxypropylcellulose; X-ray scattering; steady-state shear flow)

INTRODUCTION

The behaviour of nematic polymers under flow has attracted much attention in recent years. Of the experiments made, coupled optical and mechanical experiments have provided much information about the structures formed during flow and after the cessation of flow[1–9]. On the theoretical side, the original Doi theory[10], modified by Marrucci *et al.*[11–13], has given a convincing explanation of rheological phenomena observed with nematic polymers, such as negative normal stresses. The picture that emerges at present is the following. Two main regimes of flow exist, each relating to a range of shear rates. At low shear rates, the nematic director does not remain at a fixed orientation, but undergoes a continuous rotation, which is very complex when the initial orientation of the director is not in the shearing plane[14]. This complex director motion, called tumbling, strongly distorts the director field, which responds to this motion by creating defects in order to decrease the elastic free energy. These defects are apparent when studying the flow behaviour by light scattering[15], and the formation of defects during flow has been observed in a thermotropic polymer system[16,17]. In the latter case, the defects created during shearing consist of half-strength disclination loops lying in the shearing plane. It is clear that, in this region, the flow-induced structure depends strongly on both strain and shear rate. This structure is often called the 'domain' structure, since the complex director patterns form defect-free domain-like areas. Several workers have found direct evidence for the existence of tumbling[18,19]. Indirect evidence comes from the existence of negative normal stresses at the upper limit of the tumbling region and large recoil values of dynamic moduli[20]. The second regime occurs at higher shear rates and is called the flow-aligned regime. The director adopts a stable position in space, within the shearing plane and pointing close to the flow direction. Optical microscopy and light scattering in the flow-aligned regime show the nematic fluid to be a defect-free sample[15,21], although submicrometre defects may still be present in this regime.

Relaxation after the cessation of flow has also been studied[22–24]. Such work has shown that there is a drastic difference between the relaxation behaviour of aqueous anisotropic hydroxypropylcellulose (HPC) solutions and polypeptide solutions. Whilst the former show an increase of the dynamic modulus, G', and the dynamic loss modulus, G'', with time, the polypeptide solutions show a decrease of the moduli. Two shear regimes are found for aqueous HPC solutions. In the region where director tumbling is thought to occur, i.e. before the first normal stress becomes negative, the behaviour of G' and G'' depends on the previously applied shear rate. Moreover, the final saturation values of these moduli occur at smaller relaxation times when the shear rate is higher. However, in the flow-aligned region, the behaviour of G' and G'' reveals that the relaxation time is

* To whom correspondence should be addressed

independent of the previously applied shear rate and attains maximum values about 400 s after the cessation of shear. Optical microscopy and light scattering studies show that the defect behaviours in these two regimes are very different, with the occurrence of a special texture, known as the banded texture[25–27], as a relaxation mechanism from the flow-aligned regime.

Light scattering under flow gives information that is mainly dominated by the presence of defects. It is therefore difficult to extract the overall molecular orientation of the nematic fluid. X-ray scattering is much better adapted to this task[28–31]. In the present work, global orientation parameters are reported for four aqueous HPC liquid-crystalline solutions both during steady-state shearing and following the cessation of shear.

EXPERIMENTAL

Liquid-crystalline solutions of concentration 45%, 50%, 55% and 60% w/w HPC were prepared using HPC supplied by Aqualon (Klucel EF), having a molecular weight of 60 000[32]. The HPC powder was dried *in vacuo* at 50°C for 12 h, and then mixed thoroughly with the appropriate quantity of water to yield solutions of the required concentration by weight of HPC. The solution was allowed to stand for 24 h before finally being centrifuged at 4000 rev min^{-1} for 6 h to remove air bubbles.

X-ray diffraction measurements were performed using AXIS, a novel two-dimensional imaging system developed at Reading[33]. This system, based on a CCD (charge-coupled device) X-ray detector supplied by Photonic Science Ltd, has been successfully used with a conventional X-ray source to provide rapid access to quantitative structural information[31]. With this system and for the solutions studied, a data accumulation time of 60 to 300 s was necessary when used with a conventional laboratory-based Cu Kα sealed-tube source operating at 40 kV and 40 mA. This report details work that was conducted at the LURE synchrotron radiation source situated at Orsay, Paris, on beamline D24. When the AXIS system was used with this much more intense source, minimum accumulation times of 4 s were practicable with the HPC solutions. Beam focusing and pinhole collimation ensured a beam size of approximately 1 mm^2. The distance from the shear cell to the detector was set at 76 mm providing a scattering vector* range $0 \leq |s| \leq 1$ $Å^{-1}$ and an azimuthal scattering range, ϕ, of 0 to 360°, although some of this pattern was obscured by the beam stop and its mount.

The shear cell and the associated X-ray geometry are shown in *Figure 1*. A complete description has been given elsewhere[34]. Basically it is a plate–plate rheo-X-ray rheometer with the two plates separated by a poly(tetrafluoroethylene (PTFE) spacer; thin mica sheets are used as the windows for each plate. One plate is fixed, and the other is rotated at controlled velocities to give a shear-rate range of between 0.05 and 100 s^{-1} for the sample thickness of 2 mm used in these experiments. The use of slotted windows on the rotating plate allows transmission of X-rays throughout ~ 90% of each rotation. Since these solutions are observed to undergo a phase

* $|s| = 4\pi \sin(\theta)/\lambda$, where λ is the wavelength of the incident radiation and 2θ is the angle through which the beam is scattered

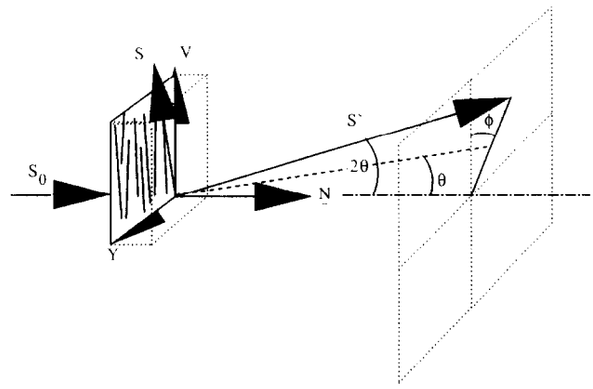

Figure 1 A schematic representation of the geometry of the X-ray rheometer. S_0 is the incident beam vector, S' is the scattered beam, 2θ is the scattering angle, α is the azimuthal angle, S is the scattering vector, V is the direction of shear, N is a normal to the plane in which the structural correlations are probed and Q is the shear gradient within the shear cell

separation at approximately 35–40°C[35] for these concentrations, temperature was maintained in the range 26.5 ± 1.5°C using a recirculating system.

Each experiment consisted of three stages. The first stage involved shearing the solution from rest at a constant shear rate for a constant time, 5 s^{-1} for 30 s; the purpose of this was to ensure that the solution was always in the same reproducible state at the start of each experiment. In the second stage, which ran continuously from the first, a selected shear rate was applied for at least 100 shear units, the minimum shear stress required to ensure that steady-state conditions have been attained[26]. In the third stage, which also ran continuously from the second, the shear was halted and the solution studied for the decay of any shear-induced effects for periods of up to 30 min. Throughout these three stages the local structure of the solutions was studied using the time-resolving X-ray scattering facility. These experiments focused on the relaxation behaviour of the global orientation following steady-state shear rates of 0.1, 0.2, 0.5, 1, 5 and 80 s^{-1}.

Diffraction data were averaged over periods of 8 s. This allowed a 10 s cycle throughout the duration of the experiments, including time for data analysis and storage. All data were corrected for absorption by the sample and the mica windows, air scattering and the effects associated with the partial polarization of synchrotron radiation. Structural changes within the sample were monitored by means of variations in the orientation parameter $\langle P_2(\cos\alpha)\rangle$, calculated from the azimuthal variation in the scattering intensity $I(\alpha)$ using standard procedures[36,37], at $|s| \sim 0.4$ $Å^{-1}$, where α is the angle between the velocity axis in the shear cell and the scattering vector. No correction was made for the fact that a flat detector cannot fully access data at $\alpha = 0$. However, since the angle of scattering is small, $2\theta \sim 10°$, this effect may be considered negligible. The orientation parameter thus obtained is the global orientation parameter $\langle P_2(\cos\alpha)\rangle_G$ within the sample, and may be considered as the product of the liquid-crystal order parameter $\langle P_2(\cos\alpha)\rangle_L$ and the liquid-crystal director distribution $\langle P_2(\cos\alpha)\rangle_D$, i.e.

$$\langle P_2(\cos\alpha)\rangle_G = \langle P_2(\cos\alpha)\rangle_D \langle P_2(\cos\alpha)\rangle_L \quad (1)$$

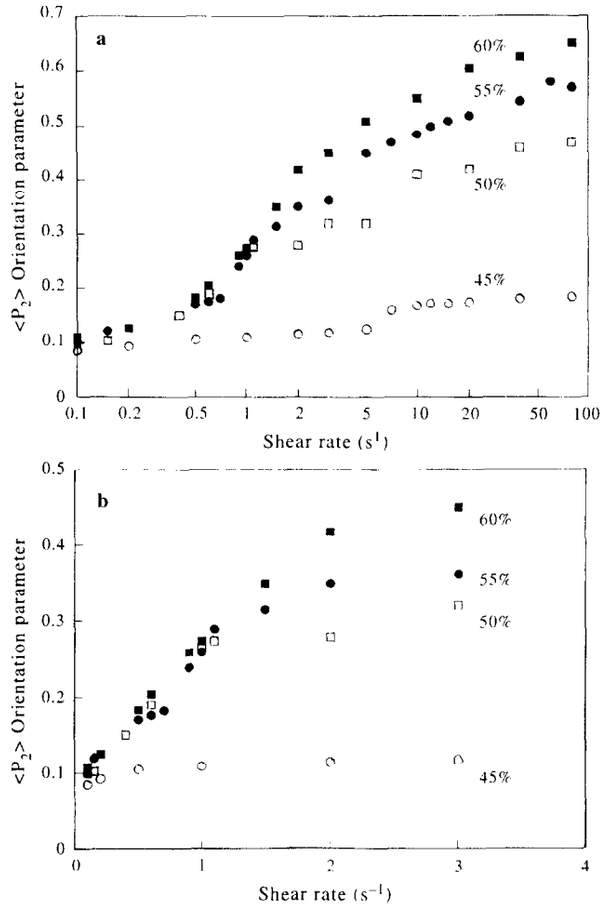

Figure 2 The measured global orientation parameter $\langle P_2(\cos\alpha)\rangle_G$ for liquid-crystalline solutions of 45%, 50%, 55% and 60% HPC in water subjected to a steady shear flow, plotted against the shear rate: (a) with the shear rate plotted on a logarithmic scale and (b) with shear rate plotted on a linear scale. There is an uncertainty of ±0.02 for each value of the orientation parameter

RESULTS

Previous X-ray scattering investigations[38] have utilized a diffractometer system to probe the static structure of HPC solutions. In these studies two diffuse peaks can clearly be seen in the scattering patterns of the anisotropic solutions. The first diffuse maximum at $s \sim 0.4\,\text{Å}^{-1}$, which arises from interactions between neighbouring HPC chains, is of primary interest. We have used the azimuthal variation in the intensity of the scattering of this peak at a fixed value of $|s|$ to evaluate the orientation parameter[31].

Steady-state flow

According to the procedure described above, the steady-state orientation parameter $\langle P_2\rangle$ has been determined for the four HPC concentrations in the shear-rate range between 0.1 and $80\,s^{-1}$ (*Figure 2*). These results are in agreement with a previously reported more limited study on 55% and 60% HPC solutions[31]. For all solutions the orientation increases with increasing shear rate, before reaching a saturation value $\langle P_2\rangle_n$ at high shear rates. At the highest shear rate the texture of the aqueous HPC solutions is close to that of a monodomain nematic fluid. In that case $\langle P_2\rangle_n$ may be equated with the intrinsic nematic order parameter, providing shear does not significantly increase the nematic order parameter. A plot of $\langle P_2\rangle_n$, deduced from the data shown in *Figure 2*, is given in *Figure 3* as a function of the solution concentration. The values are significantly lower than predicted by Doi[10] for a rod-like polymer solution, presumably due to the semi-flexible nature of HPC. The saturation effect in the orientation *versus* shear rate curves shown in *Figure 2* occurs at the same shear rate as the maximum of the first positive region of the first normal stress difference[26].

Relaxation

Figures 4 and *5* give the orientation parameter as a function of time for the 50% and 60% solutions for three different previously applied shear rates. Three basic types

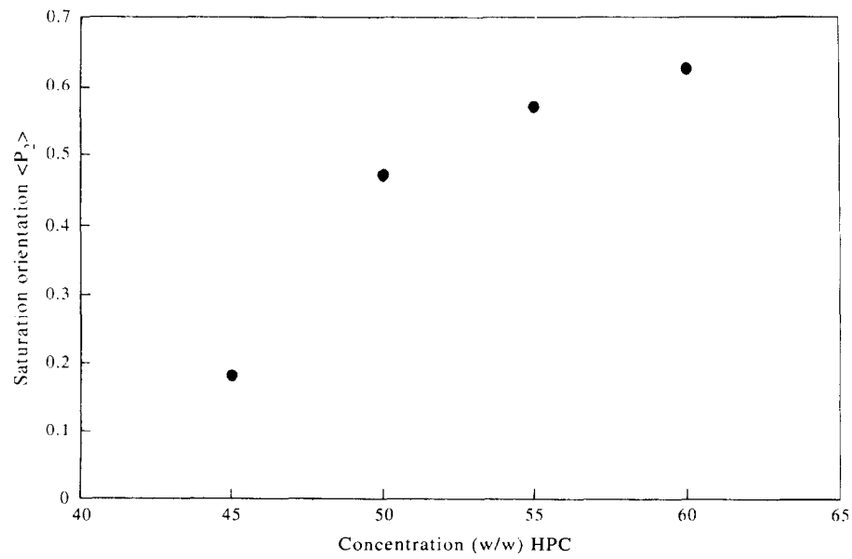

Figure 3 The saturation values of the global orientation parameter $\langle P_2\rangle_n$ obtained from the data in *Figure 1*, plotted as a function of the solution concentration. There is an uncertainty of ±0.02 for each value of the orientation parameter

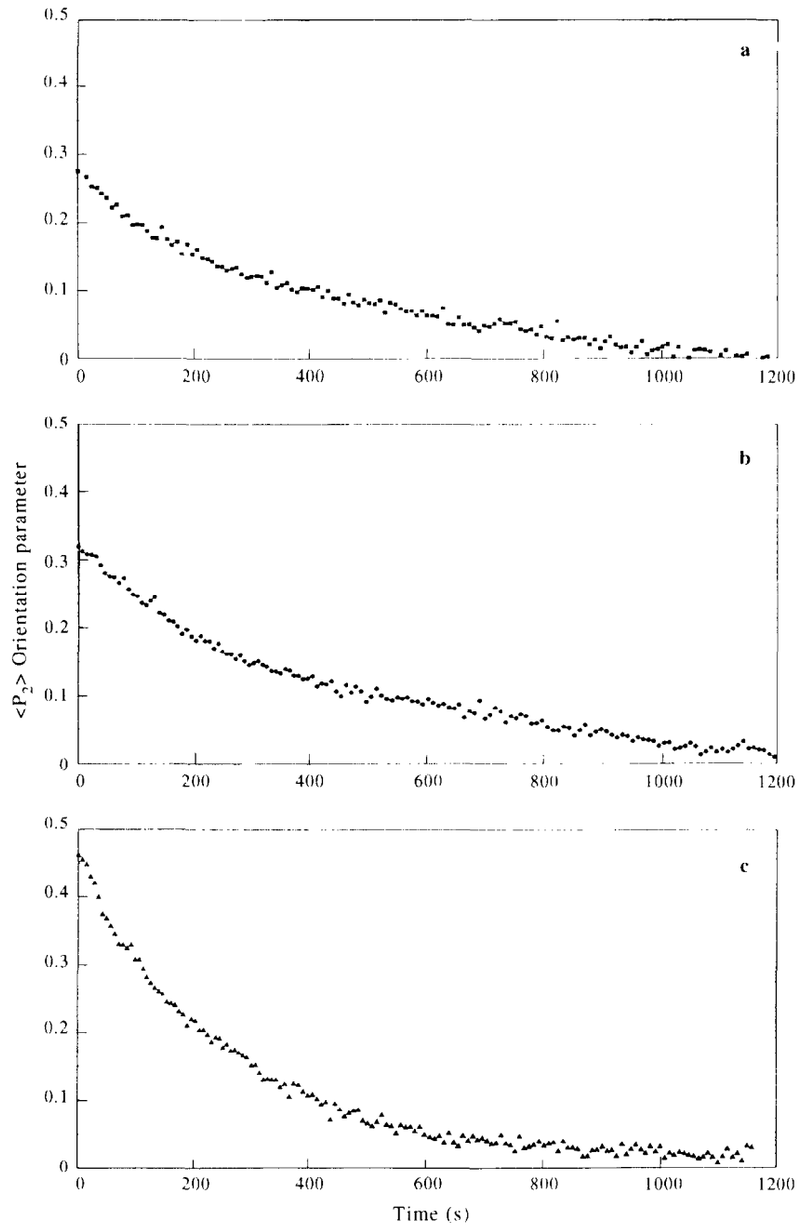

Figure 4 The decay of the measured global orientation parameter $\langle P_2(\cos\alpha)\rangle$ for a 50% solution of HPC in water as a function of time following the cessation of shear at (a) $0.5\,s^{-1}$, (b) $5\,s^{-1}$ and (c) $80\,s^{-1}$. There is an uncertainty of ± 0.02 for each value of the orientation parameter

of relaxation may be identified and particular examples are shown in semi-log plots in *Figure 6*. These three modes of relaxation have been labelled type I, type II and type III.

Type I: This is a simple exponential decay of the induced orientation to a zero value. The time constant for this relaxation is of the order of 400 s and is independent of the previous shear rate. In general it has been found that this behaviour occurs for 50% and higher-concentration solutions sheared at low shear rates, $\leq 1\,s^{-1}$, and for the 45% solution irrespective of the previous shear rate.

Type II: This type of decay exhibits two stages to the relaxation behaviour. Initially the orientation is seen to decay exponentially as in type I relaxation. However, at an intermediate orientation (which appears to be a constant for the given solution), the decay process becomes more gradual, and the remaining orientation decays over a period of hours. For this second stage the time constant is $\sim 20\,000$ s. This behaviour has been observed only in the 50% solution, when previously sheared at higher steady-state shear rates, $\geq 5\,s^{-1}$.

Type III: In this case, the initial decay is much more rapid. The time constant is between 30 and 130 s, and is inversely proportional to the previous shear rate. Thereafter the decay is similar to that observed in type II. There is an exponential decay with a time constant of between 300 and 500 s, which is followed by a transition to a much slower decay; this second stage occurs when the orientation has dropped to an intermediate level. This behaviour is limited to the most concentrated

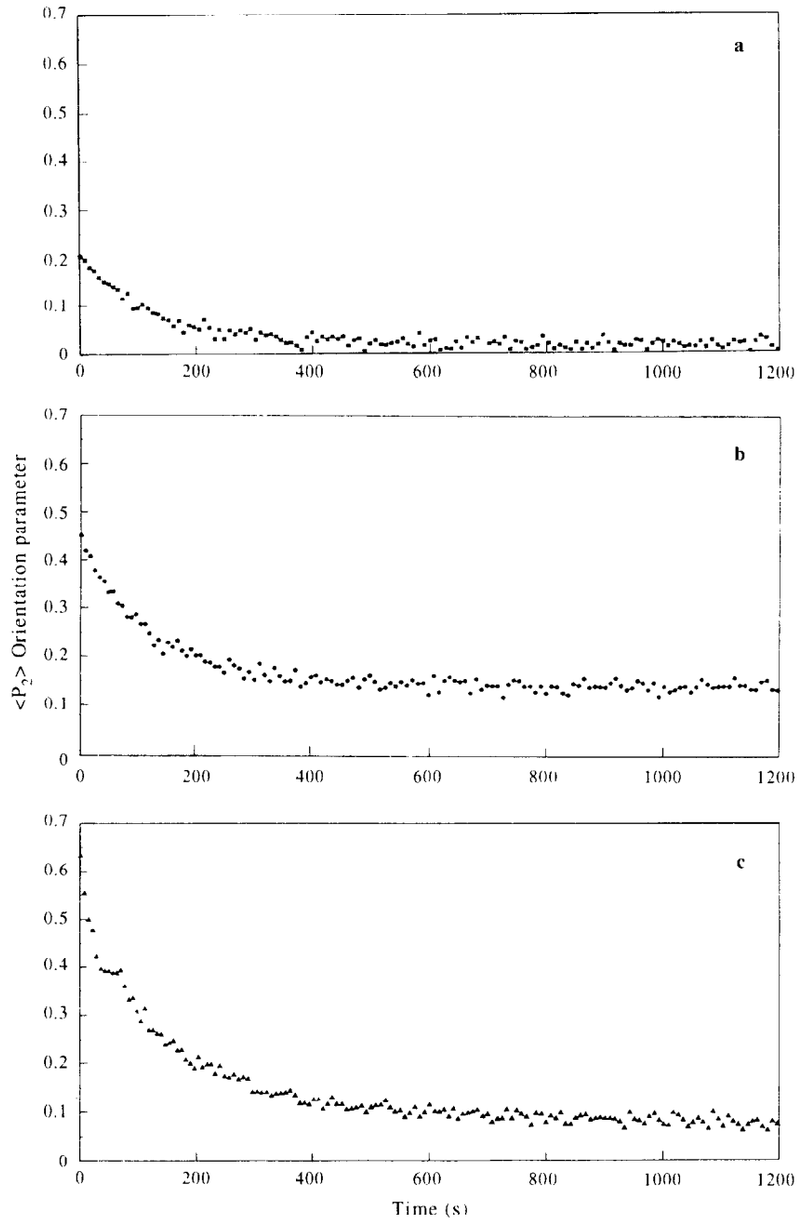

Figure 5 The decay of the measured global orientation parameter $\langle P_2(\cos\alpha)\rangle$ for a 60% solution of HPC in water as a function of time following the cessation of shear at (a) $0.5\,s^{-1}$, (b) $5\,s^{-1}$ and (c) $80\,s^{-1}$. There is an uncertainty of ± 0.02 for each value of the orientation parameter

solutions ($\geq$ 55%), sheared at the highest shear rates, $\geq 5\,s^{-1}$.

Figure 7 collates all of the data obtained in this study from the range of concentrations and shear rates. The figure provides a map of the different types of relaxation behaviour for the HPC/water system.

DISCUSSION

Steady state

The 50%, 55% and 60% HPC solutions (*Figures 2* and *3*) exhibit a development in global orientation with shear rate that has been interpreted in a previous paper[31] by a sequence of two phenomena: A first transition occurs at low shear rate from an out-of-shearing-plane tumbling to an in-shearing-plane tumbling. The second stage involves a tumbling to flow-aligning transition, which occurs at higher shear rates. This second transition is thought to take place when the first normal stress difference becomes negative[26]. The 45% solution behaves differently to that described above and does not display the banded texture following the cessation of flow[26]. This is an indication that the tumbling regime is dominant throughout the range of shear rates considered. This explains the low value for $\langle P_2\rangle_n$ observed for the 45% solution. Essentially the transition to the flow-aligned region does not occur and hence the observed value of $\langle P_2\rangle_n$ does not correspond to the intrinsic order nematic parameter.

Relaxation

For the HPC solutions studied here, the solution

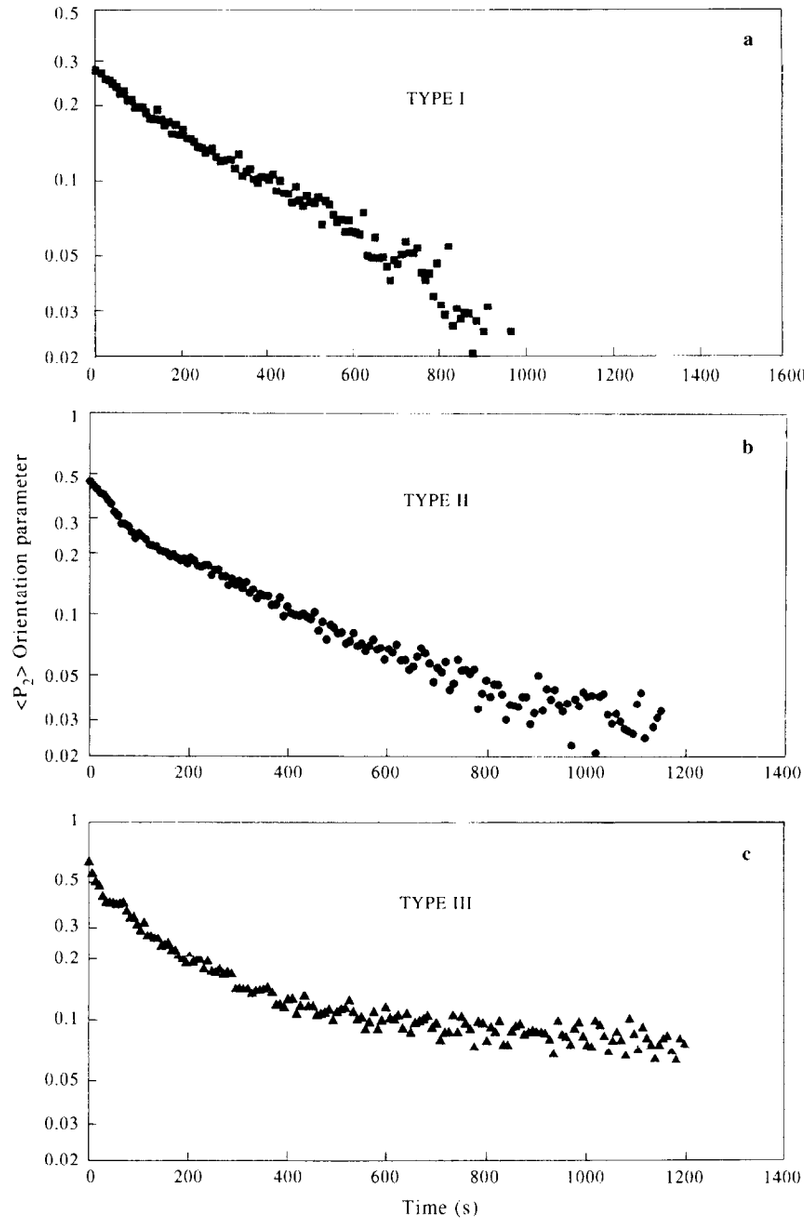

Figure 6 The measured global orientation parameter $\langle P_2(\cos\alpha)\rangle_G$ as a function of time following the cessation of steady shear. Three types of relaxation can be recognized depending upon the solution concentration and previous shear rate. One example of each type is given: (a) type I, 50% from $1\,s^{-1}$; (b) type II, 50% from $80\,s^{-1}$; and (c) type III, 60% from $80\,s^{-1}$. There is an uncertainty of ± 0.02 for each value of the orientation parameter

concentration and the previous shear history play an important role in determining the type of decay in orientation following the cessation of shear. From this observation it follows that the morphology of the system during steady-state shear is important in determining the relaxation behaviour upon the cessation of shear. It is apparent that the type of behaviour in the steady-state flow, that is either tumbling or flow-aligned, has an influence on the type of decay that occurs when shear is halted. The nature of the regime controls the level of orientation that is present in the fluid during steady-state shear. For example, the tumbling region gives a low global orientation parameter. The key factor thus appears to be the level of orientation induced during steady-state shearing. An examination of the data in *Figures 2* and *7* reveals a strong correlation between the level of induced orientation and the subsequent relaxation behaviour recorded. For example, type I decay was only observed when the value of the steady-state $\langle P_2\rangle$ was below 0.3. Type II decay was observed only when the steady-state orientation parameter lay between 0.3 and 0.5, and type III decay occurred when the $\langle P_2\rangle$ was greater than 0.5.

In order to relate these observations to the microscopic and macroscopic processes that occur during relaxation, it is essential to consider the scale over which orientation measurements are made. Liquid-crystalline polymers consist of regions in which there is a high degree of orientational order, even in the absence of an

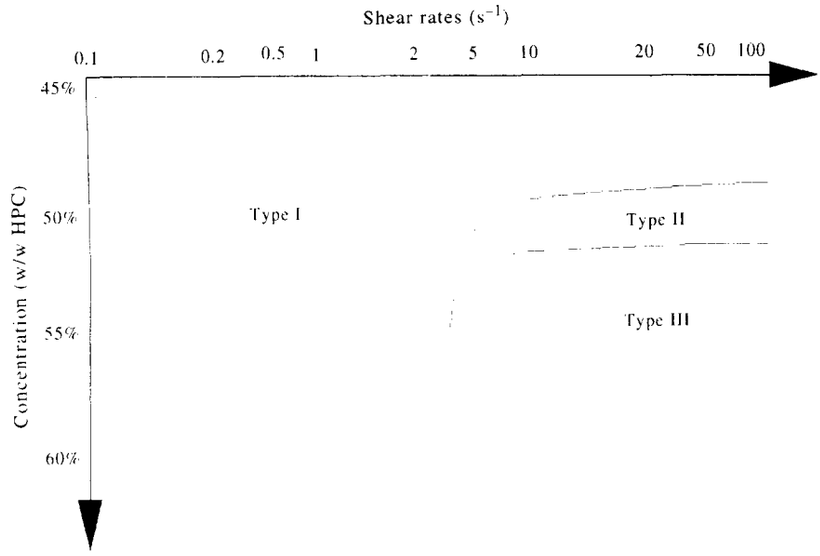

Figure 7 A schematic diagram showing the sensitivity of the relaxational behaviour of anisotropic HPC solutions to the solution concentration and previous shear

external field. These regions are bounded by defects, so that the size of these regions is usually of the order of 1–2 μm. Each region can be ascribed an external director and a local order parameter that describes the level of preferred orientation within that area. On a much larger scale, these defects form a complex network throughout the sample. The presence of these defects ensures that in the absence of an external field the external directors will exhibit no preferred global orientation. It has previously been reported[31] that the effect of shear is to induce an increase in the global orientation within a sample. A complex interplay between the creation of defects (the defect density increases in the tumbling region[39]) and elongation of defects (the global orientation increases) takes place until the onset of the flow-aligning regime, which strongly decreases the defect density. In the tumbling region, where a large number of defects are present, the behaviour of the relaxation is of type I. The defect network, only slightly distorted by the flow[39], will return to its initial macroscopic disordered state. In light scattering experiments[15,39], the slightly elliptical pattern under flow transforms during relaxation into the circular pattern found at rest. The mechanism that can be imagined is that defects will slightly elongate and relax. Such a relaxation will have a time constant independent of the previous shear rate, as observed. If this relaxation arises through a director rotation from one defect to another, as assumed previously in order to minimize the distortion energy[40], we have:

$$\tau = \left(\frac{\eta}{K\rho}\right) \tag{2}$$

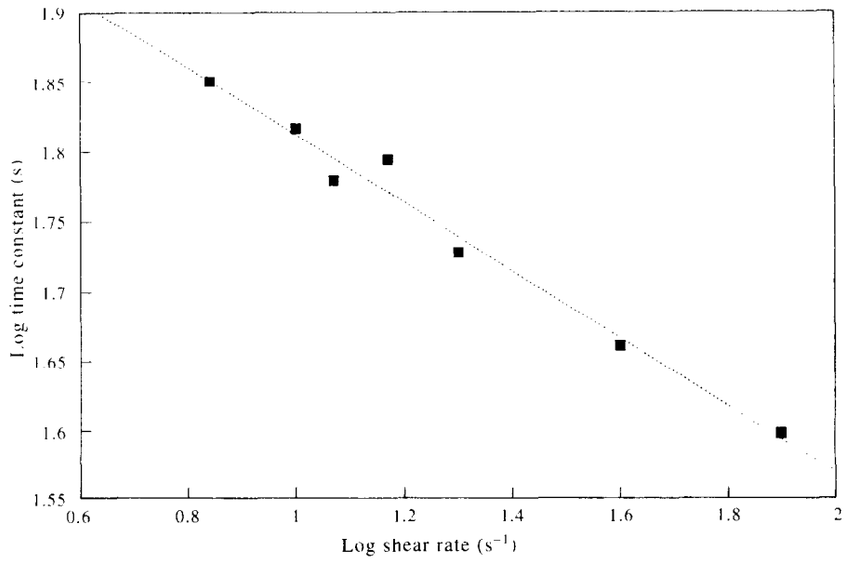

Figure 8 The logarithm of the time constant observed in the type III relaxation of a 55% solution of HPC in water plotted against the logarithm of the previous shear rate

where K is an effective Frank elastic constant, ρ is the defect density, τ is the relaxation time and η is an effective viscosity. Equation (2) is obtained by balancing elastic and viscous forces[40]. At low shear rates K and ρ do not depend on the shear rate[40] and we can expect η to be independent of the shear rate. Thus the relaxation time τ should be a constant in this low-shear-rate regime, as observed in this study.

Types II and III correspond to the region where the depolarized small-angle light scattering patterns are transformed into a four-lobe plus a bright streak pattern[3,9]. The SALS data have been interpreted as the region where elongated defect loops are present in the shearing plane. It is also in this shear-rate region that relaxation following cessation of shear produces the banded texture. The banded texture appears after an induction time of between 0 and 70 s, depending on the previous shear rate[26], and lasts for a few minutes depending on the viscosity of the solution and the previous shear rate (e.g. 120 s for a shear rate of $3\,s^{-1}$). The initial decay of orientation in types II and III relaxation occurs during the timespan of this relaxation phenomenon involving the banded texture.

At these high shear rates, the structure of the fluid is modified so profoundly that the nematic polymer will keep a memory of the steady-state orientation rather than the initial polymer structure prior to shear flow. The relaxation does not lead to the same texture found at rest, but keeps an 'equilibrium' degree of orientation, the value of which depends upon the previous shear rate (see *Figure 5* at shear rates of 5 and $80\,s^{-1}$). This may explain the different 'equilibrium' values found when measuring G' and G'' (refs. 22, 41).

During the initial stage of the relaxation for type III behaviour, the time constant is inversely related to the previous shear rate. *Figure 8* shows a plot of the time constant against the shear rate. The log–log plot gives an exponent of -0.5 ± 0.02. An inverse dependence of a characteristic relaxation time on the previous shear rate has also been observed previously[20,41]. Rheological curves often scale this region on the product of the time and previous shear rate.

CONCLUSION

We have utilized a novel X-ray area detection system at a synchrotron radiation source to investigate the changes in the global orientation parameter as a means of quantifying the response of a lyotropic liquid-crystalline solution during both steady-state flow and subsequent relaxation following the cessation of flow. The relaxation behaviour following the cessation of shear is strongly dependent upon the level of orientation that develops during shearing. It correlates well with what is known about the flow mechanisms of such nematic polymer fluids. X-ray scattering has been shown to be ideal for studying time-dependent effects in these complex anisotropic fluids.

ACKNOWLEDGEMENTS

This work forms part of a UK (British Council)–France Alliance programme between the Polymer Science Centre, Reading, and the Ecole des Mines, Sophia Antipolis. It was supported in part by the Science and Engineering Research Council (UK) through GR/F08405 and a CASE studentship for PK with Courtaulds Research. Hydroxypropylcellulose samples were kindly provided by Aqualon, a Hercules Inc. Company, Wilmington, Delaware, USA. The experiment at LURE, Orsay, Paris, was performed as part of an EC Large Scale Facility Program and we thank Dr C. Bourgeau for her assistance at LURE.

REFERENCES

1 Asada, T., Toda, K. and Onogi, S. *Mol. Cryst. Liq. Cryst.* 1981, **68**, 231
2 Asada, T. and Onogi, S. *Polym. Eng. Rev.* 1983, **3**, 323
3 Ernst, B., Navard, P., Hashimoto, T. and Takebe, T. *Macromolecules* 1990, **23**, 1370
4 Hsiao, B. S., Stein, R. S., Deutscher, K. and Winter, H. H. *J. Polym. Sci., Polym. Phys. Edn.* 1990, **28**, 1571
5 Kiss, G. and Porter, R. S. *Mol. Cryst. Liq. Cryst.* 1980, **60**, 267
6 Moldenaers, P., Fuller, G. and Mewis, J. *Macromolecules* 1989, **22**, 960
7 Navard, P. and Zachariades, A. E. *J. Polym. Sci., Polym. Phys. Edn.* 1987, **25**, 1089
8 Picken, S. J., Aerts, J., Doppert, H. L., Reuvers, A. J. and Northolt, M. G. *Macromolecules* 1991, **24**, 1366
9 Takebe, T., Hashimoto, T., Ernst, B., Navard, P. and Stein, R. S. *J. Chem. Phys.* 1990, **92**, 1386
10 Doi, M. *J. Polym. Sci., Polym. Phys. Edn.* 1981, **19**, 229
11 Marrucci, G. and Maffettone, P. L. *Macromolecules* 1989, **22**, 4076
12 Marrucci, G. *Rheol. Acta* 1990, **29**, 523
13 Marrucci, G. *Macromolecules* 1991, **24**, 4176
14 Larson, R. G. and Ottinger, H. C. *Macromolecules* 1991, **24**, 6270
15 Riti, J. B. and Navard, P. *Synth. Polym. J.* 1994, **1**, 1
16 De'Neve, T., Kléman, M. and Navard, P. *C. R. Acad. Sci. Paris* 1993, **316**, 1037
17 De'Neve, T., Navard, P. and Kléman, M. *Macromolecules* 1995, **28**, 1541
18 Burghardt, W. R. and Fuller, G. G. *Macromolecules* 1991, **24**, 2546
19 Srinivasarao, M. and Berry, G. C. *J. Rheol.* 1991, **35**, 379
20 Larson, R. G. and Mead, D. W. *J. Rheol.* 1989, **33**, 1251
21 Larson, R. G. and Mead, D. W. *Liq. Cryst.* 1993, **15**, 151
22 Grizzuti, N., Moldenaers, P., Mortier, M. and Mewis, J. *Rheol. Acta* 1993, **32**, 218
23 Hongladorham, K. and Burghardt, W. R. *Macromolecules* 1993, **26**, 785
24 Moldenaers, P. and Mewis, J. *J. Non-Newtonian Fluid Mech.* 1993, **34**, 359
25 Navard, P. *J. Polym. Sci., Polym. Phys. Edn.* 1986, **24**, 435
26 Ernst, B. and Navard, P. *Macromolecules* 1989, **22**, 1419
27 Marrucci, G., Grizzuti, N. and Buonaurio, A. *Mol. Cryst. Liq. Cryst.* 1992, **153**, 263
28 Feijoo, J. L., Odell, J. A. and Keller, A. A. *Polym. Commun.* 1990, **31**, 42
29 Picken, S. J., Aerts, J., Visser, R. and Northolt, M. G. *Macromolecules* 1990, **23**, 3849
30 Nicholson, T. M., Mackley, M. R. and Windle, A. H. *Polymer* 1992, **33**, 434
31 Keates, P., Mitchell, G. R., Peuvrel-Disdier, E. and Navard, P. *Polymer* 1993, **34**, 1316
32 'Hydroxypropylcellulose: Chemical and Physical Properties', Hercules Inc., Wilmington, Delaware, 1981
33 Keates, P. and Mitchell, G. R. J. J. Thomson Physical Laboratory Technical Report 0006-92, University of Reading, 1992
34 Keates, P., Mitchell, G. R., Riti, J. B., Peuvrel-Disdier, E. and Navard, P. *J. Non-Newtonian Fluid. Mech.* 1994, **52**, 197
35 Werbowyj, R. S. and Gray, D. G. *Macromolecules* 1980, **13**, 69

36 Lovell, R. and Mitchell, G. R. *Acta. Cryst allogr. (A)* 1980, **37**, 135
37 Mitchell, G. R. and Windle, A. H. in 'Developments in Crystalline Polymers–2' (Ed. D. C. Bassett), Applied Science, London, 1988
38 Keates, P., Mitchell, G. R. and Peuvrel-Disdier, E. *Polymer* 1992, **33**, 3517
39 Riti, J. B. and Navard, P. in preparation
40 De'Neve, T., Kléman, M. and Navard, P. *Liquid Crystals* 1994, **18**, 67
41 Grizzuti, N., Cavella, S. and Cicarelli, P. *J. Rheol.* 1990, **34**, 1293